MULTI-MODALITY EXPANSION AND RETENTION FOR LLMS THROUGH PARAMETER MERGING AND DECOUPLING

Anonymous authors
Paper under double-blind review

ABSTRACT

Extensive fine-tuning of the synthesis between multimodal encoders and Large Language Models (LLMs) on modality-specific data can expand the modalities that LLM can handle, leading to the formation of Multimodal Large Language Models (MLLMs). However, this paradigm to expanding modalities heavily relies on initiating fine-tuning from scratch with new multimodal data, which is both resource-intensive and inflexible. In this paper, we propose *MMER (Multi-modality Expansion and Retention)*, a novel *training-free* approach that reuses and composes existing MLLMs to facilitate effective multimodal expansion while retaining the original performance of each MLLM. In particular, MMER maintains the multimodal encoders of the MLLMs while merging their LLM parameters. By comparing the original LLM parameters with the merged ones, MMER can create binary masks that enable an approximate separation of the LLM parameters for each modality. This process allows the decoupled parameters to independently process modality-specific inputs, thereby reducing parameter conflicts and maintaining the fidelity of the original MLLMs. Additionally, MMER integrates strategies to prevent catastrophic forgetting by employing a similar approach to separately decouple the parameters fine-tuned on new tasks from the original parameters. Experiments on three multimodal tasks and fourteen dual-modal tasks show significant improvements over recent baselines, demonstrating that MMER can effectively expand multimodal capabilities of LLMs while retaining 99.6% of the original performance. Further experiments in both single-task and cross modalities multi-task scenarios reveal that MMER significantly mitigates catastrophic forgetting.

1 INTRODUCTION

Large Language Models (LLMs) (Kenton & Toutanova, 2019; Touvron et al., 2023; Wu et al., 2023b) have recently become a cornerstone in artificial intelligence due to their exceptional performance. Building upon the capabilities of LLMs, researchers (Li et al., 2023b; Liu et al., 2023; Bai et al., 2023) integrate encoders for additional modalities and utilize extensive modality-text data for alignment. These integrated systems are then fine-tuned to develop Multimodal Large Language Models (MLLMs), which excel at processing multimodal information. This paradigm has led to the successful creation of numerous MLLMs across various modalities (Wu et al., 2024; Jiang et al., 2023).

Most MLLMs are specialized in dual modalities, with examples including vision-oriented LLMs like LLaVA (Liu et al., 2023) and MiniGPT-4 (Zhu et al., 2024b), as well as video LLMs (Lin et al., 2023; Maaz et al., 2024) and audio LLMs (Chu et al., 2023; Deshmukh et al., 2023). Despite these advancements, there is a growing impetus to expand the number of modalities that MLLMs can handle in order to address diverse applications. A straightforward method involves adding multiple new modality encoders or employing a unified multimodal encoder, followed by re-fine-tuning the MLLMs with fresh modality-text data. For instance, X-LLMs (Chen et al., 2023a) and MACAW-LLMs (Lyu et al., 2023) integrate encoders for images, videos, and audio with an LLM simultaneously, while OneLLM (Han et al., 2024) connects a universal encoder that handles eight distinct modalities with an LLM. These different architectures are then aligned and fine-tuned using new multimodal instruction data (e.g., image-speech chat). However, this kind of method lacks flexibility because it requires fine-tuning from scratch on new modality-text data to expand the multimodal capabilities

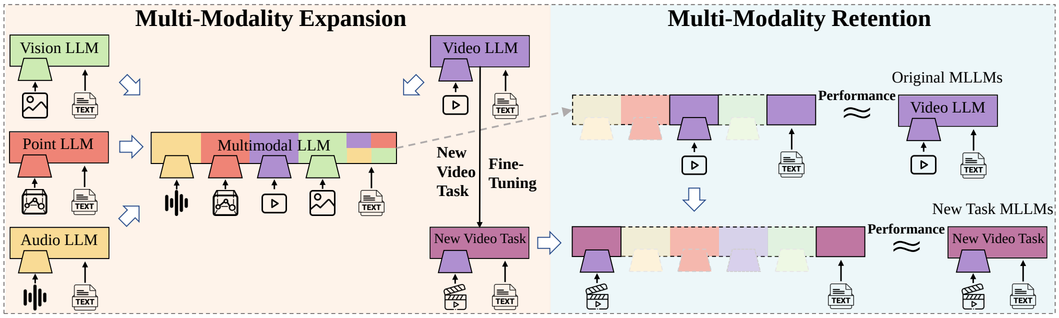

Figure 1: Illustration of the key idea of our MMER approach. Multi-Modality Expansion creates a versatile model from existing MLLMs through a **training-free and extensible** process. Multi-Modality Retention reconstructs the original MLLMs or new task MLLMs to retain their performance and mitigate catastrophic forgetting.

of MLLMs. Moreover, it necessitates the generation or acquisition of high-quality multimodal instruction data (Zhao et al., 2023), consuming substantial computational and human resources.

To overcome the aforementioned limitations, researchers have explored model merging or composition (Chen et al., 2024; Shukor et al., 2023; Panagopoulou et al., 2023) to facilitate multimodal expansion in MLLMs. For instance, Chen et al. (2024) proposed NaiveMC, a basic, training-free framework that reuses and combines modality-specific encoders from multiple MLLMs into the merged LLM, enabling it to handle multiple modalities. They further introduced the DAMC framework (Chen et al., 2024), which retrains existing MLLMs by separating modality parameters from language model parameters. This approach mitigates parameter interference in the merged MLLM, thereby enhancing the performance of multimodal expansion. However, these two frameworks encounter a trade-off: NaiveMC is train-free but delivers lower performance, whereas DAMC, though requiring training, yields better results. Nevertheless, both frameworks share a common drawback: they struggle to retain the original modality performance of the MLLMs due to parameter interference.

In this paper, we propose a novel training-free approach named MMER (Multi-modality Expansion and Retention), which achieves multimodal expansion while bypassing the trade-off of previous methods and retains the performance of each original MLLM (See Figure 1). First, we merge the *task vectors* (Ilharco et al., 2023), which represent the difference between the fine-tuned parameters and the pre-train LLM parameters, into a single merged task vector. Next, by comparing the Directional Congruence and Dominant Significance of the merged task vector with the original task vectors, we construct modality-specific binary masks. These masks effectively identify the modality-specific information retained in the merged task vector and approximately decouple it back into the original modality parameters without requiring additional training. This decoupling strategy enables the merged MLLM to independently process non-textual modality information using its corresponding reconstructed parameters, thereby significantly reducing interference from other modalities.

Additionally, by re-adding the decoupled modality task vectors back to the base LLM parameters and integrating the corresponding encoders, we are able to reconstruct the original MLLMs approximately. This strategy not only retains the performance of the original modalities but also saves storage space. Remarkably, our MMER approach exhibits strong resistance against catastrophic forgetting (Yang et al., 2023; Goodfellow et al., 2013) when handling new tasks. It can enhance performance on new tasks without diminishing effectiveness on previous tasks. The process begins with selecting the corresponding original MLLM based on the modality of the new task for fine-tuning. Then, the task vector of the newly fine-tuned MLLM is merged with the task vectors of all original MLLMs to create a merged task vector, and a corresponding mask is generated. This strategy effectively separates the parameters of the new task from the original parameters, thereby preventing damage to the original parameters during fine-tuning and significantly mitigating catastrophic forgetting.

We demonstrated the effectiveness of our MMER approach by composing four MLLMs (i.e., image, audio, video, and point cloud) and conducted extensive experiments across three scenarios. Firstly, in benchmarks like MCUB (Chen et al., 2024), which involve more than two modalities, MMER achieves a significant improvement compared to NaiveMC framework and various model merging methods such as TA (Ilharco et al., 2023) and TIES (Yadav et al., 2023). This confirms that MMER realizes and enhances the multimodal expansion capabilities of LLMs without requiring additional training. Secondly, we examined the performance of MLLMs approximately reconstructed by MMER on fourteen dual-modal benchmarks covering four modalities. The experiments reveal that these MLLMs fully retain their original performance. Lastly, we verified MMER's resistance to catastrophic forgetting in both single-task and cross modalities multi-task scenarios. Our results show that MMER retained 98% of its performance on previous tasks while efficiently adapting to new tasks.

In summary, our work makes several significant **contributions**: (i) We propose a training-free MMER approach that enables seamless multimodal expansion for LLMs through multimodal parameter merging and decoupling. (ii) We demonstrate two additional practical applications of the MMER approach: retaining the performance of original MLLMs and mitigating catastrophic forgetting in MLLMs. (iii) We conduct extensive and rigorous experiments on various multimodal benchmarks across three scenarios, and the experimental results confirm the effectiveness of the MMER approach.

2 Related Work

2.1 Multimodal Large Language Models

As text-based LLMs are insufficient to meet evolving demands, significant research (Dai et al., 2023; Li et al., 2023a; Achiam et al., 2023; Ye et al., 2023) efforts are focused on developing LLMs that can effectively handle multimodal inputs. Vision LLMs (Alayrac et al., 2022; Li et al., 2023b; Liu et al., 2023), as trailblazers in this field, have excelled across numerous vision-language tasks by connecting pre-trained visual encoders to LLMs through various alignment layers. Similarly, other modalities like audio (Rubenstein et al., 2023; Deshmukh et al., 2023) and video (Lin et al., 2023; Maaz et al., 2024) have rapidly followed suit, resulting in a surge of dual-modality MLLMs. Meanwhile, researchers have explored unifying multiple modalities into a single LLM. Approaches like Pandagpt (Su et al., 2023) and ImageBind-llm (Han et al., 2023) connect a unified multimodal encoder like ImageBind (Girdhar et al., 2023) with an LLM but rely only on image-text data, leading to suboptimal performance. OneLLM (Han et al., 2024) improves on this by introducing a versatile encoder for eight modalities and aligning all of them with language. However, these methods cannot expand modalities due to the encoders have fixed input modalities. Another approach connects multiple modality-specific encoders to an LLM, as seen in X-LLM (Chen et al., 2023a) and MACAW-LLM (Lyu et al., 2023), which integrate encoders for images, videos, and audio. AnyMAL (Moon et al., 2023) further adds an IMU encoder. These methods typically require high-quality multimodal data for joint training and still struggle with modality expansion. In contrast, our MMER approach provides an efficient, training-free solution for seamless multimodal expansion in LLMs.

2.2 Model Merging and Model Composition

The proliferation of various model checkpoints has sparked concerns over data privacy and resource efficiency, shifting focus toward model merging and composition (Yang et al., 2024; Lu et al., 2024). Model merging, which merges multiple models fine-tuned from the same initialization, can improve single-task performance (Gupta et al., 2020; Wortsman et al., 2022), out-of-distribution generalization (Arpit et al., 2022; Ramé et al., 2022), or combine their capabilities (Wan et al., 2024; Ilharco et al., 2022). For example, TA (Ilharco et al., 2023) defines the concept of task vectors and uses arithmetic operations like addition to merge models. TIES (Yadav et al., 2023) mitigates interference during merging by pruning redundant parameters and resolving sign conflicts, while DARE (Yu et al., 2024) proposes a preprocessing step that randomly drops and scales parameters to achieve the same goal. TALL-masks (Wang et al., 2024) proposes an algorithm to identify original task information from the merged task vector and eliminate harmful parameters to enhance merging performance. Model merging has been further applied to multimodal models (Aiello et al., 2024; Wu et al., 2023a). Sung et al. (2023) and Sundar et al. (2024) investigated merging multimodal transformers to improve performance in specific tasks, such as speech recognition. Model Tailor (Zhu et al., 2024c) merges the original model with a fine-tuned model to mitigate catastrophic forgetting in MLLMs. However, they do not explore the merging of multiple MLLMs. The NaiveMC and DAMC frameworks (Chen et al., 2024) address this by using model merging and composition to create a unified MLLM that inherits the modality capabilities of multiple MLLMs, thus enabling seamless expansion into new modalities. Nonetheless, each framework has its limitations: one necessitates additional training, while the other delivers subpar performance. In contrast, MMER approach avoids both of these drawbacks. It enhances the multimodal expansion capabilities of MLLMs

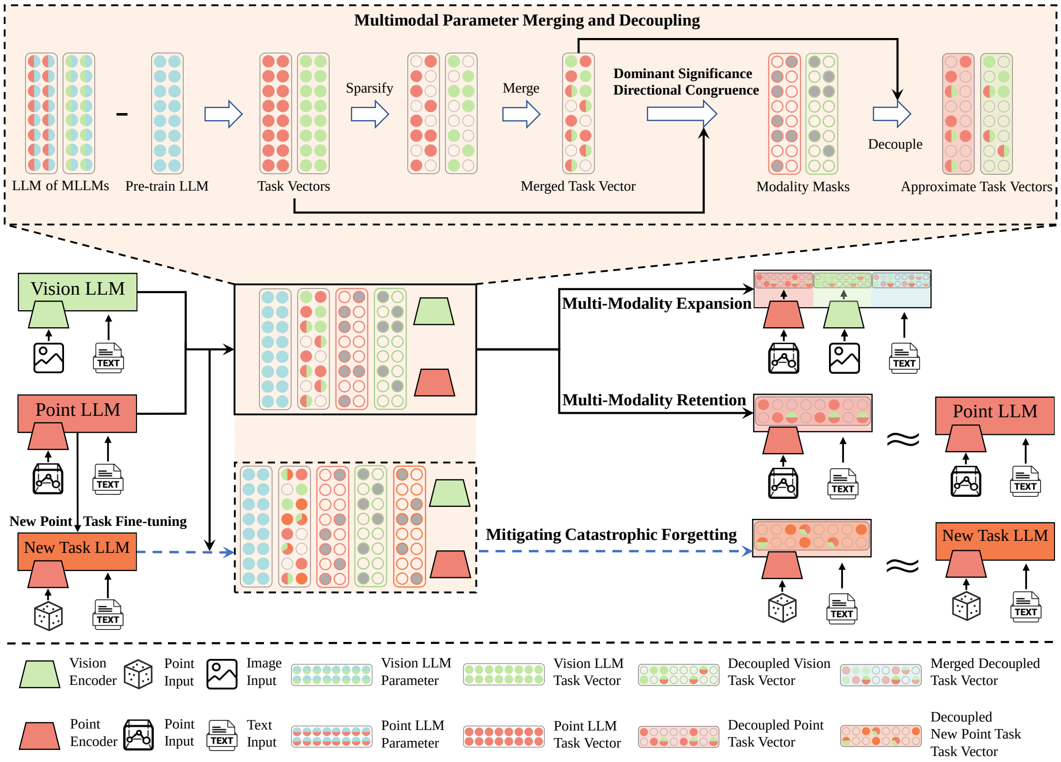

Figure 2: Illustration of the details of our MMER approach with only **Image** and **Point Cloud** modalities are considered **for clarity**. Each block corresponds to the same weight matrix, with empty blocks denoting zero value. The symbol "≈" signifies similar performance. We separate modality-specific components from the base fine-tuned LLMs, then apply parameter merging and decoupling to these LLMs to generate masks and merged task vector. Different task vectors are decoupled to reconstruct original MLLMs based on the specific scenario.

without requiring additional training, while nearly retaining the original modalities' performance. Additionally, it demonstrates impressive resistance to catastrophic forgetting when adapting to new tasks. Appendix A provides a detailed comparison of MMER approach with related methods.

3 Methodology

In our MMER approach, we first merge the LLM parameters $\{\theta_1, \theta_2, \ldots, \theta_n\}$ from multiple MLLMs, all fine-tuned from the same base LLM θ_{pre}, into a unified LLM. However, such a merged model is particularly susceptible to interference between parameters from different modalities, which can degrade the performance of modality-specific representations. To overcome this challenge, we adopt a training-free parameter decoupling method to effectively enhance the multimodal performance of the merged LLM while also ensuring that the performance of each original modality is retained. This method approximately decouples modality-specific parameters within the merged parameter, ensuring that the representation of each non-text modality is processed independently by their respective parameters. A visual workflow illustrating our MMER approach is depicted in Figure 2.

3.1 Multimodal Parameter Merging and Decoupling

The key idea of the MMER approach is its mechanism of the training-free multimodal parameter merging and decoupling. Specifically, we commence by employing the advanced model merging technique Ties (Yadav et al., 2023) to merge $\{\theta_1, \theta_2, \ldots, \theta_n\}$. Ties first calculates the task vectors for each MLLM as $\tau_{i,pre} = \theta_i - \theta_{\text{pre}}$. Subsequently, it refines these task vectors $\tau_{i,pre}$ by selecting the Top $K\%$ extreme values to filter out non-essential parameters, which yields sparse task vectors τ_i. These sparse task vectors are then merged according to sign consistency to generate the merged task vector $\tau_* = \text{merge}(\sum_{i=1}^{n} \tau_i)$ and the final merged LLM parameter is $\theta_* = \theta_{\text{pre}} + \alpha \cdot \tau_*$, where $\alpha > 0$

is a scaling factor determined by the accuracy of the validation dataset. This dataset is constructed by selecting one task from each modality and combining their respective validation sets.

Previous studies (Panigrahi et al., 2023; Wang et al., 2024) have shown that after merging multiple different task vectors, the majority of their parameter information is retained and embedded into the resulting merged task vector τ_*. By comparing the original MLLM task vectors τ_i with the merged task vector τ_*, we can identify the relevant parameter subsets specific to each original modality task vector. This enables the construction of modality-specific binary masks m_i, which allow decoupling and approximating of the parameters for the original modality task vectors $m_i \circ \tau_*$. These binary masks filter out irrelevant parameters in the merged task vector, preserving only modality-specific information and reconstructing the original model parameters $\hat{\theta}_i$:

$$\hat{\theta}_i = \theta_{\text{pre}} + m_i \circ \tau_* \approx \theta_i \tag{1}$$

We construct the binary masks m_i by minimizing the Manhattan distance ℓ_1^* between the reconstructed model parameters $\hat{\theta}_i$ and the LLM parameters θ_i of original MLLMs:

$$\underset{m_i \in \{0,1\}^P}{\arg\min} \left| \hat{\theta}_i - \theta_i \right| = \underset{m_i \in \{0,1\}^P}{\arg\min} \left| m_i \circ \tau_* - \tau_i \right| = \underset{m_i \in \{0,1\}^P}{\arg\min} \sum_{p=1}^{P} \left| m_i^{(p)} \circ \tau_*^{(p)} - \tau_i^{(p)} \right| \tag{2}$$

where P represents the total number of parameters. If the sign of $\tau_i^{(p)}$ is inconsistent with that of $\tau_*^{(p)}$, i.e., $\text{sign}(\tau_i^{(p)}) \neq \text{sign}(\tau_*^{(p)})$, the binary masks $m_i^{(p)}$ is set to 0 to avoid directional conflict. This step is referred to as **Directional Congruence**. Conversely, when the sign of $\tau_i^{(p)}$ aligns with $\tau_*^{(p)}$ and $\left|\tau_i^{(p)}\right| \geq \left|\tau_*^{(p)} - \tau_i^{(p)}\right|$, i.e., $\left|\tau_i^{(p)}\right| \geq 50\% \left|\tau_*^{(p)}\right|$, this indicates that $\tau_i^{(p)}$ is a dominant component of the merged parameter $\tau_*^{(p)}$. Thus, $\tau_*^{(p)}$ can be approximated as $\tau_i^{(p)}$, and $m_i^{(p)}$ is set to 1, which we refer to as **Dominant Significance**. Additionally, we introduce a scaling factor λ_i to refine the selection process of Dominant Significance to accommodate the varying numbers and modalities of original MLLMs. A smaller λ_i results in the selection of more parameters. The choice of λ_i is guided by validation dataset accuracy, enabling different masks m_i to be assigned with different values of λ_i. The final mask m_i is constructed using the following formula:

$$m_i = \begin{cases} 1 & \text{if } |\tau_i^{(p)}| \geq \lambda_i \cdot 50\% |\tau_*^{(p)}| \text{ and } \text{sign}(\tau_i^{(p)}) = \text{sign}(\tau_*^{(p)}) \\ 0 & \text{otherwise} \end{cases} \tag{3}$$

Our subsequent experiments validate the effectiveness of this parameter decoupling strategy. As illustrated in Figure 4, by employing binary masks to separate the pertinent subset of critical parameters, the original parameters can be approximately decoupled, thereby retaining the original performance.

3.2 The MMER Approach

We now present a comprehensive exposition of how the aforementioned multimodal parameter merging and decoupling method not only facilitates both the multi-modality expansion and retention but also addresses the challenge of catastrophic forgetting in MLLMs.

3.2.1 Multi-Modality Expansion

Typical MLLMs are composed of two key elements: modality-specific components, including modality encoders and alignment layers, and a base fine-tuned LLM. Our MMER approach begins by disentangling these components. MMER proceeds by applying the multimodal parameter merging and decoupling strategy to these base fine-tuned LLMs of multiple MLLMs, yielding a merged task vector τ_*, the pre-trained LLM parameter θ_{pre}, and n modality-specific binary masks m_i. The corresponding modal-specific components, including their weights, are retained and reutilized directly, enabling the merged MLLM to seamlessly process all original modalities without loss of functionality.

As depicted in Figure 3, upon receiving multimodal data, MMER initially identifies the pertinent modality-specific components according to the data type and respectively encodes them into representation inputs $X = [X_{M_1}, \ldots, X_{M_n}, X_t]$, where X_{M_i} and X_t represent the modality-specific sequences and text sequences. MMER then dynamically decouples the approximate modality-specific parameters $\theta_{\text{pre}} + m_i \circ \tau_*$, adeptly separating the parameters for each modality. This crucial step ensures that non-text modality representations are processed independently with their corresponding modality parameters. It is noteworthy that text representations are processed with the merged parameter $\theta_{\text{pre}} + \overline{m} \circ \tau_*$, where $\overline{m}$ represents the average of all modality-specific masks m_i. For example, when the representations progress to the attention mechanism at the l-th layer, MMER first decouples the modality-specific parameter weights $W^Q_{*,l}$ of the queries weights in the l-th layer from τ_*, before proceeding with the subsequent computation:

$$\mathbf{Q}_l = \left[X_{M_1,l}\left(m^Q_{1,l} \circ W^Q_{*,l} + W^Q_{pre,l}\right), \dots, X_{t,l}\left(\overline{m}^Q_l \circ W^Q_{*,l} + W^Q_{pre,l}\right)\right] \tag{4}$$

where $W^Q_{pre,l}$ represents the weights of the queries in the l-th layer form θ_{pre}. Subsequently, MMER sequentially decouples the modality-specific parameters for the keys and values in the l-th layer, and executes the computations to derive $\mathbf{K}_l$ and $\mathbf{V}_l$. Following this, we carry out the attention operation:

$$X^a_l = Attention(\mathbf{Q}_l, \mathbf{K}_l, \mathbf{V}_l) \tag{5}$$

$$[X^a_{M_1,l}, \dots, X^a_{M_n,l}, X^a_{t,l}] = Split(X^a_l) \tag{6}$$

Please note that the output representation should be partitioned according to the different modalities to match the input form. Consequently, the final output of the attention mechanism at the l-th layer is:

$$[X^o_{M1,l}, \dots, X^o_{t,l}] = \left[X^a_{M_1,l}\left(m^O_{1,l} \circ W^O_{*,l} + W^O_{pre,l}\right), \dots, X^a_{t,l}\left(\overline{m}^O_l \circ W^O_{*,l} + W^O_{pre,l}\right)\right] \tag{7}$$

Such an implementation effectively alleviates parameter conflicts across different modalities, thereby ensuring that the merged MLLM can maintain relative fidelity when processing multimodal data.

3.2.2 Multi-modality Retention

Previous studies, such as model merging (Ilharco et al., 2023; Yadav et al., 2023) and NaiveMC (Chen et al., 2024), have demonstrated that performance tends to degrade (See Table 2) when handling the original tasks, primarily due to the discrepancies between the merged model parameter and the original model parameters. However, MMER effectively circumvents this issue, ensuring the original MLLMs' performance is retained. When dealing with tasks that are specific to the modalities of the original MLLMs, MMER can directly reconstruct an approximate version of the original MLLMs to perform inference on these tasks. The procedure is as follows: First, decouple the modality-specific task vector $m_i \circ \tau_*$ from the merged task vector, then add it to the pre-trained LLM parameter θ_{pre} to obtain the restored LLM $\hat{\theta}_i = \theta_{\text{pre}} + m_i \circ \tau_*$. Finally, integrate the corresponding modality-specific components with the restored LLM to construct the final reconstructed MLLM. This strategy effectively mitigates interference from parameters of other MLLMs and retains the original performance of each MLLM. Subsequent experiments, as illustrated in Table 2 validate the effectiveness of this strategy.

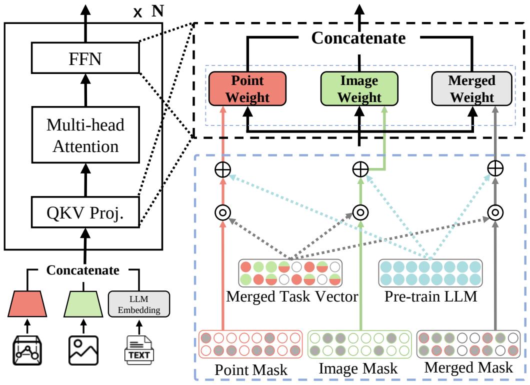

Figure 3: Details of dynamic parameter decoupling in MMER for handling multimodal data. ⊚ and ⊕ represent the Hadamard product and addition operation.

3.2.3 Mitigating Catastrophic Forgetting

Typically, fine-tuning MLLMs on new data enhances their performance on newly introduced tasks, but it often comes at the cost of diminished performance on the previous tasks (Goodfellow et al., 2013). This degradation in performance, referred to as catastrophic forgetting, arises when fine-tuning for new tasks. Drawing on the insight that most parameter information from individual task vectors is retained in the merged task vector, we can leverage MMER to additionally mitigate catastrophic forgetting. Specifically, we first select the corresponding original MLLM based on the modality of the new task and proceed to fine-tune its LLM using the new data, while keeping the modality-specific components frozen. Next, we apply the parameter merging and decoupling method to the fine-tuned MLLM, alongside all original MLLMs, generating a new merged task vector and modality- or task-specific binary masks. For the new task, we apply the task-specific mask to recover the fine-tuned MLLM for processing. For the previous tasks, we maintain the use of the previously proposed multi-modality expansion or retention strategy. This method enables MMER to effectively adapt to new tasks while retaining its performance on previous tasks, thereby substantially mitigating the risk of catastrophic forgetting.

Table 1: Accuracy (%) results on multimodal benchmarks with different combinations of video (V), image (I), audio (A), point cloud (P), and text (T) inputs. MCUB and MUSIC-AVQA consist of five and three subsets, respectively. TA and TIES serve as alternatives to the average merging method utilized in NaiveMC framework. Optimal results are highlighted in boldface, while sub-optimal results are underlined.

Task (→)	**ModelNet40**	**MUSCI-AVQA**			**MCUB**					Avg
Method (↓)	PI-T	IA-T	VI-T	VA-T	AVI-T	AVP-T	AIP-T	VIP-T	AVIP-T	
NaiveMC[ACL24] (Chen et al., 2024)	60.53	39.31	47.65	47.40	53.64	56.28	60.53	54.60	59.16	53.23
TA[ICLR23] (Ilharco et al., 2023)	62.04	40.22	47.97	46.70	53.44	56.28	63.36	55.40	59.72	53.90
TIES[NeurIPS23] (Yadav et al., 2023)	61.74	43.27	49.27	48.60	53.64	55.47	61.74	54.60	58.55	54.10
NaiveMC (w/ DARE[ICML24] (Yu et al., 2024))	60.32	39.78	47.98	47.67	53.64	56.68	60.73	54.80	59.53	53.46
TA (w/ DARE)	**62.75**	40.46	47.98	46.92	54.25	56.48	64.17	55.40	60.08	54.27
TIES (w/ DARE)	61.96	43.78	49.54	48.98	54.25	55.87	62.55	55.20	59.06	54.57
MMER (ours)	62.15	**47.25**	**51.27**	**51.77**	**56.48**	**59.31**	**65.59**	**56.00**	**61.63**	**56.82**

4 Experiments Setup

4.1 Implementation

In our forthcoming experiments, we explored our MMER approach across four MLLMs: Image, Audio, Video, and Point Cloud LLMs, all built upon Vicuna-7B-v1.5 (Zheng et al., 2023). To ensure fairness and comparability in our analysis, we fine-tuned these four MLLMs in the same environment, following previous works (Liu et al., 2024; Lin et al., 2023; Xu et al., 2024; Panagopoulou et al., 2023). Details regarding the fine-tuning of these MLLMs are provided in Appendix B.2. For the hyperparameters in the parameter merging and decoupling process, we set α to 1 and K to 80%, while λ was calibrated according to the different modalities.

4.2 Baseline Methods

In the multi-modality expansion and retention experiments, we first compared MMER with the training-free modal composition framework NaiveMC (Chen et al., 2024). We excluded the comparison with DAMC framework (Chen et al., 2024), as its reliance on additional training introduces variables that could compromise the fairness of our experimental evaluation. Additionally, since model merging methods can substitute the average merging strategy in NaiveMC framework to enhance multimodal performance, we also compared against training-free model merging baselines, including TA (Ilharco et al., 2023) and TIES (Yadav et al., 2023). Given that DARE (Yu et al., 2024) is complementary to other model merging methods, we combined it with TA, TIES, and NaiveMC framework in our experiments. Additionally, we included the zero-shot performance of the original MLLMs as a performance upper bound. We evaluated the performance based on both the evaluation scores or accuracy and the performance retention, the latter of which is defined in Appendix B.1.

4.3 Datasets and Benchmarks

In the multi-modality expansion experiments, we evaluated several multimodal benchmarks containing more than two modalities, including MCUB (Chen et al., 2024), MUSIC-AVQA (Li et al., 2022), and ModelNet40 (Wu et al., 2015) with images. Furthermore, we assessed the multi-modality retention across fourteen dual-modal benchmarks spanning four modalities: image, video, audio, and point cloud. Specifically, the image tasks include VQAv2 (Goyal et al., 2017), GQA (Hudson & Manning, 2019), TextVQA (Singh et al., 2019), VizWiz (Gurari et al., 2018), ScienceQA (Lu et al., 2022), POPE (Li et al., 2023c), and OK-VQA (Marino et al., 2019). The audio tasks cover TUT (Mesaros et al., 2017), VocalSound (Gong et al., 2022), and Clotho (Drossos et al., 2020). The video benchmarks include MSRVTT (Xu et al., 2016) and MSVD (Chen & Dolan, 2011), while the point cloud tasks focus on ModelNet40 (Wu et al., 2015) and Objaverse (Deitke et al., 2023). Finally, we evaluated MMER's resilience to catastrophic forgetting in both single-task and cross modalities multi-task settings across two new tasks, Flickr30k (Young et al., 2014) and Clotho-AQA (Lipping et al., 2022).

5 Main results

Multi-Modality Expansion. Table 1 summarizes the primary results of the multi-modality expansion experiments across four benchmarks. The notation "XY-T" denotes the combination of modalities included in the dataset, where A stands for Audio, P for Point Cloud, V for Video, I for Image, and T for Text. For example, "IA-T" signifies that the dataset comprises Image, Audio, and Text modalities. Regardless of the input data modalities, we utilized the unified MLLM, derived from merging MLLMs across four distinct modalities, to process the data. We can draw the following observations: **(i)** Various advanced model merging methods improve the performance of the NaiveMC framework, suggesting that training-free model merging methods can still be effectively applied to the merging of MLLMs. This is a domain that has not been previously explored. Additionally, this implies that there are considerable parameter conflicts in the merged MLLM, as

Table 2: Results on fourteen dual-modal benchmarks spanning four modalities. The performance retention from the original MLLMs are shown in parentheses. Original MLLMs refer to their zero-shot results. “Trimmed Avg” represents the average result obtained after excluding three point or audio classification tasks.

Task (→)	**2 Point Tasks**	**3 Audio Tasks**	**2 Video Tasks**	**7 Image Tasks**	**Trimmed Avg**
Method (↓)	Score (%) / Acc.(%)	Score (%) / Acc.(%)	Acc.(%)	Acc.(%)	Score (%) / Acc.(%)
Original MLLMs	23.15 / 21.27	25.30 / 24.71	39.79	62.23	24.23 / 51.01
NaiveMC [ACL2024] (Chen et al., 2024)	22.65 $_{(97.8)}$ / 20.49 $_{(96.3)}$	24.59 $_{(97.2)}$ / 30.65 $_{(124.8)}$	36.92 $_{(93.0)}$	52.56 $_{(83.6)}$	23.62 $_{(97.5)}$ / 44.59 $_{(88.3)}$
TA [ICLR23] (Ilharco et al., 2023)	22.96 $_{(99.2)}$ / 21.02 $_{(98.8)}$	24.68 $_{(97.5)}$ / 31.88 $_{(129.8)}$	37.57 $_{(94.5)}$	54.89 $_{(87.5)}$	23.82 $_{(98.3)}$ / 46.23 $_{(91.0)}$
TIES [NeurIPS23] (Yadav et al., 2023)	22.82 $_{(98.6)}$ / 20.83 $_{(97.9)}$	24.79 $_{(98.0)}$ / 32.15 $_{(130.9)}$	37.81 $_{(95.1)}$	54.10 $_{(86.2)}$	23.80 $_{(98.3)}$ / 45.96 $_{(90.6)}$
NaiveMC (w/ DARE[ICML2024] (Yu et al., 2024))	22.83 $_{(98.6)}$ / 20.77 $_{(97.6)}$	24.72 $_{(97.7)}$ / 31.62 $_{(128.8)}$	37.63 $_{(94.4)}$	53.61 $_{(85.3)}$	23.78 $_{(98.1)}$ / 45.62 $_{(89.8)}$
TA (w/ DARE)	23.04 $_{(99.5)}$ / 21.25 $_{(99.9)}$	24.82 $_{(98.1)}$ / 32.44 $_{(132.0)}$	37.52 $_{(94.4)}$	55.47 $_{(88.4)}$	23.95 $_{(98.8)}$ / 46.50 $_{(91.4)}$
TIES (w/ DARE)	22.76 $_{(98.3)}$ / 20.98 $_{(98.6)}$	24.92 $_{(98.5)}$ / 33.02 $_{(134.4)}$	38.00 $_{(95.6)}$	54.73 $_{(87.2)}$	23.84 $_{(98.4)}$ / 46.37 $_{(91.4)}$
MMER (ours)	**23.14** $_{(99.9)}$ **/ 22.49** $_{(105.7)}$	**25.20** $_{(99.6)}$ **/ 38.51** $_{(155.6)}$	**39.28** $_{(98.5)}$	**62.40** $_{(100.3)}$	**24.17** $_{(99.8)}$ **/ 50.84** $_{(99.4)}$

Table 3: Results on previous and new tasks in the single-task scenario and **cross-modalities** multi-task scenario. MMER-xx refers to merging the MLLM fine-tuned on a new task xx into MMER. MMER-Clotho-AQA+Flickr30k denotes the merging of both the audio LLM fine-tuned on Clotho-AQA and the vision LLM fine-tuned on Flickr30k into MMER. The symbol "(∼)" signifies performance retention.

Task (→)	**Previous Tasks**					**New Tasks**	
	2 Point tasks	3 Audio tasks	2 Video tasks	7 Image tasks	3 Multimodal tasks	Clotho-AQA	Flickr30k
Baseline (↓)	Score / Acc.	Score / Acc.	Acc.	Acc.	Acc.	Acc.	Score
Original MLLMs	23.15 / 21.27	25.30 / 24.71	39.79	62.23	-	49.40	51.26
Fine-tune on Clotho-AQA	-	19.82 / 12.31 (↓)	-	-	-	57.80 (↑)	-
Fine-tune on Flickr30k	-	-	-	57.25 (↓)	-	-	57.71 (↑)
MMER	23.14 / 22.49	25.20 / 38.51	39.28	62.40	56.82	49.28	51.00
MMER-Clotho-AQA	22.95 / 21.87	25.12 / 38.23 (∼)	39.17	62.20	56.53	57.71 (↑)	50.94
MMER-Flickr30k	23.05 / 22.03	24.96 / 37.68	38.90	62.27 (∼)	56.44	48.94	57.08 (↑)
MMER-Clotho-AQA+Flickr30k	22.82 / 21.56	24.88 / 37.69 (∼)	38.53	61.94 (∼)	55.89	57.52 (↑)	56.72 (↑)

these methods primarily focus on mitigating conflicts among merging parameters. **(ii)** Our proposed MMER approach significantly outperforms NaiveMC across all input combinations and tasks. This demonstrates that MMER effectively extends multimodal capabilities and enhances the merged MLLMs' ability to manage these modality combinations without requiring additional training for each specific combination. **(iii)** Furthermore, MMER achieves superior performance on all tasks, except for ModelNet40, when compared with model merging methods. This indicates that directly decoupling parameters after merging is more effective than merely reducing parameter conflicts during the merging process. **(iv)** We observe that as the number of merging modalities increases, the relative accuracy improvement of TIES (w/ DARE) compared to NaiveMC diminishes (i.e., from 4.81% to 0.94% to -0.17%), indicating that mutual interference among merging parameters intensifies. However, although the relative accuracy improvement of MMER declines, it remains significant (i.e., from 9.00% to 5.21% to 4.17%), indicating that parameter decoupling remains effective despite severe parameter conflicts.

Multi-Modality Retention. To evaluate how effectively each method retains the performance of the original MLLMs, we conducted experiments across tasks corresponding to the original MLLMs. The results are recorded in Table 2, where we observe the following: **(i)** Interestingly, all methods demonstrate substantial performance improvements on specific audio and point cloud tasks, which we attribute to task-specific differences. Specifically, these tasks, TUT, VocalSound, and ModelNet40, are all classification tasks, whereas the others involve captioning or question-answering tasks. The original audio and point cloud LLMs are not fine-tuned for classification tasks, resulting in their failure to follow instructions and leading to poorer zero-shot performance in these tasks. However, parameter merging unlocks their ability to follow instructions, as the training data for the vision LLM included similar instructions. This resulted in performance improvements even when the merged parameter is decoupled. To account for the impact of these tasks, we additionally provide the average performance trimming these tasks in Table 2 for a more accurate comparison of the various methods. **(ii)** Although NaiveMC successfully achieves multimodal expansion for handling multimodal tasks, its performance on the original tasks shows a substantial deviation from that of the original MLLMs. While varied model merging methods can partially alleviate the decline in original performance, the gap remains significant. In contrast, our MMER almost completely retains the original performance. For instance, in the trimmed average performance, our method attains 99.8% and 99.4% performance retention of the original MLLMs' evaluation scores and accuracy, respectively. Detailed performance for each task is provided in Appendix D.2.

Mitigating Catastrophic Forgetting. Finally, Table 3 illustrates that MMER effectively alleviates catastrophic forgetting, whether in single-task or multi-task scenarios across different modalities. **(i)** Clotho-AQA represents an audio task, while Flickr30k represents a visual task. Thus, we fine-tuned the original audio LLM and vision LLM separately on the respective new task. We observe that while fine-tuning MLLMs improves performance on new tasks, it tends to degrade performance on previous tasks in the corresponding modalities. In contrast, the MMER approach, which additionally incorporates a fine-tuned MLLM (i.e., MMER-Clotho-AQA and MMER-Flickr30k), demonstrates strong robustness. It maintains nearly the original performance across various previous tasks and adapts effectively to new tasks, achieving results comparable to those of fine-tuned MLLMs.

Table 4: Performance retention & Storage vs. Mitigating MLLMs' catastrophic forgetting methods in the **same modality**. Let N, P, and P' represent the number of new tasks, the total LLM parameters, and the modality-specific component parameters, assuming each float parameter occupies 32 bits.

Method	**One New Task**		**Two New Tasks**		**Storage**
	Previous tasks	New task	Previous tasks	New tasks	
Model Tailor[ICML24] (Zhu et al., 2024c)	96.47 %	91.69 %	99.28 %	87.50 %	$32(P + P')$
MMER (ours)	**99.86 %**	**99.67 %**	**99.63 %**	**99.42 %**	$64P + 32P' + NP$

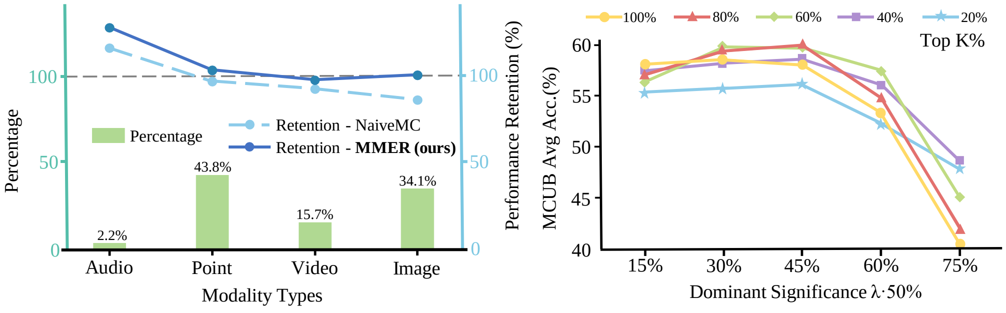

(a) (b)

Figure 4: **(a).** The bar plot illustrates the percentage of parameters selected by different modality masks, while the lines depict the performance retention of NaiveMC and the MLLMs reconstructed by MMER across various dual-modal benchmarks. **(b).** The line plots depict the variations in MCUB average accuracy across different merging sparsity ratios (Top $K\%$) and Dominant Significance ($\lambda \cdot 50\%$).

(ii) Additionally, we integrated both fine-tuned MLLMs into the MMER approach together to showcase its performance in cross modalities multi-task scenario. As the number of integrating MLLMs increases, MMER continues to maintain performance across various new and previous tasks to some extent. However, its ability to preserve performance does slightly diminish. Detailed performance for each task is provided in Appendix D.2.

In Table 4, we compare our MMER approach with the latest method for mitigating catastrophic forgetting in MLLMs within the same modality, since Model Tailor (Zhu et al., 2024c) is unable to accommodate new tasks across different modalities. The results show that MMER consistently outperforms Model Tailor in both single-task and multi-task scenarios, highlighting its effectiveness. Furthermore, as the number of new tasks increases, MMER maintains relatively stable performance, whereas Model Tailor exhibits a significant decline in performance on new tasks (i.e., from 91.69% to 87.50%), despite some improvement on previous tasks. However, a minor drawback of MMER is that its storage cost is approximately twice that of Model Tailor. Nonetheless, as the number of new tasks grows, MMER's practicality becomes more pronounced, making it a more viable solution in scenarios where balancing performance and storage efficiency is crucial.

6 Additional Results and Analysis

Modality-Specific Masks Analysis. Figure 4 (a) illustrates the percentage of parameters selected by different modality masks and compares the performance retention of MLLMs reconstructed with MMER against NaiveMC. It can be observed that MMER outperforms NaiveMC across all four modalities, with performance that is close to or even exceeds the original levels. This indicates that all integrated knowledge is preserved after merging, and the parameter subsets selected by the masks retain crucial modality-specific information. Additionally, we find that the audio mask, despite retaining only 2.2% of the parameters, still contributes to performance improvement. This finding is consistent with previous research (Yu et al., 2024), which noted that "Supervised fine-tuned language models tend to acquire excessively redundant delta parameters (also known as task vectors)." Our results further confirm that this observation holds true for MLLMs as well.

Hyperparameters Analysis. Figure 4 (b) explores the impact of the hyperparameters Top $K\%$ and the scaling factor λ in multimodal parameter merging and decoupling. Firstly, Top $K\%$ controls the sparsity of the original task vectors. When sparsity is excessively high (e.g., 20% or 40%), performance deteriorates markedly due to the insufficient information retained in the sparse parameters. Conversely, in the absence of sparsity (e.g., 100%), the method fails to mitigate parameter conflicts among the original parameters, thereby hindering the approximate decoupling of modality parameters. The effect of the scaling factor λ is akin to that of Top $K\%$. Specifically, the scaling factor λ regulates the extent of information that the mask extracts from the merged task vector. If λ is set too high, the decoupled modality parameters will contain insufficient effective information, leading to performance collapse (e.g., 60% or 75%). Conversely, if λ is too low (e.g., 15%), irrelevant parameters remain, resulting in poor performance. In summary, Top $K\%$ and the scaling factor λ work in tandem to regulate the amount of effective information contained in the decoupled parameters. For instance, the performance with K set to 60% and λ to 30% closely mirrors the results when K is set to 80% and λ to 45%.

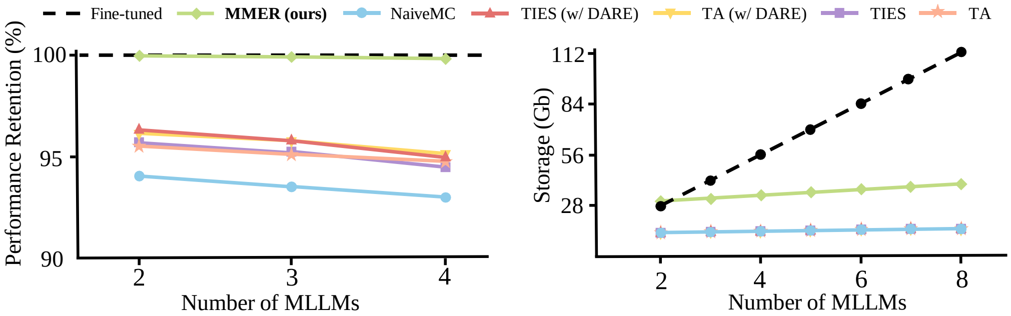

Figure 5: Performance retention and Storage cost vs. Number of original MLLMs in multi-modality retention experiments. Our MMER approach can nearly retain the initial performance across various combinations of MLLMs while significantly compressing the fine-tuned checkpoints.

Performance & Storage vs. MLLM Quantity. Finally, Figure 5 presents the performance retention and storage costs of merging varying numbers of MLLMs in multi-modality retention experiments. Our observations suggest that as the number of merging MLLMs increases, performance declines across all methods. This indicates that as more MLLMs are merged, conflicts between the merging parameters intensify. Nevertheless, our MMER consistently outperforms model merging methods, experiencing only minor performance degradation. In contrast, model merging methods exhibit a noticeable performance drop when dealing with multiple MLLMs. This highlights that parameter decoupling is robust in effectively mitigating parameter conflicts.

Although model composition or merging methods maintain low storage costs that remain constant regardless of the number of merging MLLMs, their lower performance may constrain their practical applicability. In contrast, maintaining individual MLLMs preserves strong performance for their respective modalities but fails to achieve multimodal expansion and results in linear growth in storage costs. Our MMER approach strikes an effective balance between these approaches. It enables multimodal expansion while retaining nearly 100% of the original MLLMs' modality capabilities and provides additional resilience against catastrophic forgetting. Moreover, it significantly reduces storage costs, as shown in Figure 5. Storage comparison details are in Appendix C.

Ablation Study. We conducted ablation experiments on the parameter decoupling steps to evaluate their effectiveness. In Table 5, we begin with the original parameter decoupling strategy and systematically remove components such as Directional Congruence, Dominant Significance, and the scaling factor λ. We then report the performance of MMER in both multi-modality expansion and retention scenarios. Removing Directional Congruence means that parameters are selected solely based on Dominant Significance, i.e., $m_i = 1\{\ |\tau_i| \geq 50\% \cdot \lambda_i|\tau_*|\}$. Removing Dominant Significance entails retaining parameters solely based on the consistency of their signs, i.e., $m_i = 1\{sign(\tau_i) = sign(\tau_*)\}$. Table 5 shows that the steps in parameter decoupling are crucial for optimizing performance. Specifically, Directional Congruence proves to be the most critical. Without it, the decoupled parameters are almost meaningless and lose all the original modality information. Next in importance is Dominant Significance. Without filtering out crucial parameters, irrelevant ones persist and significantly interfere with the original parameters. Finally, the scaling factor λ also plays a role, causing performance degradations of 4.93% in multi-modality expansion experiments and 4.92% in retention experiments.

Table 5: Ablation study on all steps of parameter decoupling. In retention experiments, we excluded three point and audio classification tasks.

Method	**3 Expansion Tasks**	**11 Retention Tasks**
	Avg ACC.	**Avg Score (%) / Avg ACC. (%)**
MMER	**56.82**	**24.17** $_{(\mathbf{99.8})}$ **/ 50.84** $_{(\mathbf{99.4})}$
– Directional Congruence	7.20	10.05 $_{(41.6)}$ / 8.34 $_{(16.7)}$
– Dominant Significance	33.87	14.71 $_{(60.5)}$ / 28.93 $_{(57.1)}$
– Scaling Factor λ	54.02	23.14 $_{(95.6)}$ / 47.78 $_{(93.9)}$

7 Conclusion

In this paper, we propose a novel training-free approach MMER that reuses and composes existing MLLMs to resolve the dilemma faced by MLLMs during multimodal expansion: costly retraining or suboptimal performance. MMER retains multimodal encoders and merges LLM parameters, constructing binary masks to decouple modality-specific parameters. This innovative mechanism enables independent handling of modality-specific inputs by their respective parameters, thereby significantly reducing parameter conflicts to enhance multimodal performance. Additionally, MMER can reconstruct the original MLLMs by integrating decoupled parameters with the base LLM, effectively retaining the original performance. Finally, by incorporating fine-tuned MLLMs for new tasks into MMER approach, it isolates the parameters for new tasks from the original ones, thus mitigating catastrophic forgetting. Extensive experiments have validated the effectiveness and robustness of MMER. We hope this work inspires further exploration of training-free multimodal expansion for LLMs.

REFERENCES

Josh Achiam, Steven Adler, Sandhini Agarwal, Lama Ahmad, Ilge Akkaya, Florencia Leoni Aleman, Diogo Almeida, Janko Altenschmidt, Sam Altman, Shyamal Anadkat, et al. Gpt-4 technical report. *arXiv preprint arXiv:2303.08774*, 2023.

Emanuele Aiello, Lili Yu, Yixin Nie, Armen Aghajanyan, and Barlas Oguz. Jointly training large autoregressive multimodal models. In *Proceedings of the International Conference on Learning Representations (ICLR)*, 2024.

Jean-Baptiste Alayrac, Jeff Donahue, Pauline Luc, Antoine Miech, Iain Barr, Yana Hasson, Karel Lenc, Arthur Mensch, Katherine Millican, Malcolm Reynolds, et al. Flamingo: a visual language model for few-shot learning. In *Advances in Neural Information Processing Systems (NeurIPS)*, 2022.

Devansh Arpit, Huan Wang, Yingbo Zhou, and Caiming Xiong. Ensemble of averages: Improving model selection and boosting performance in domain generalization. In *Advances in Neural Information Processing Systems (NeurIPS)*, 2022.

Jinze Bai, Shuai Bai, Shusheng Yang, Shijie Wang, Sinan Tan, Peng Wang, Junyang Lin, Chang Zhou, and Jingren Zhou. Qwen-vl: A frontier large vision-language model with versatile abilities. *arXiv preprint arXiv:2308.12966*, 2023.

Chi Chen, Yiyang Du, Zheng Fang, Ziyue Wang, Fuwen Luo, Peng Li, Ming Yan, Ji Zhang, Fei Huang, Maosong Sun, and Yang Liu. Model composition for multimodal large language models. In *Proceedings of the Annual Meeting of the Association for Computational Linguistics (ACL)*, 2024.

David L. Chen and William B. Dolan. Collecting highly parallel data for paraphrase evaluation. In *Proceedings of the Annual Meeting of the Association for Computational Linguistics (ACL)*, pp. 190–200, 2011.

Feilong Chen, Minglun Han, Haozhi Zhao, Qingyang Zhang, Jing Shi, Shuang Xu, and Bo Xu. X-llm: Bootstrapping advanced large language models by treating multi-modalities as foreign languages. *arXiv preprint arXiv:2305.04160*, 2023a.

Sanyuan Chen, Yu Wu, Chengyi Wang, Shujie Liu, Daniel Tompkins, Zhuo Chen, Wanxiang Che, Xiangzhan Yu, and Furu Wei. Beats: Audio pre-training with acoustic tokenizers. In *Proceedings of the International Conference on Machine Learning (ICML)*, volume 202, pp. 5178–5193, 2023b.

Yunfei Chu, Jin Xu, Xiaohuan Zhou, Qian Yang, Shiliang Zhang, Zhijie Yan, Chang Zhou, and Jingren Zhou. Qwen-audio: Advancing universal audio understanding via unified large-scale audio-language models. *arXiv preprint arXiv:2311.07919*, 2023.

Wenliang Dai, Junnan Li, Dongxu Li, Anthony Meng Huat Tiong, Junqi Zhao, Weisheng Wang, Boyang Li, Pascale Fung, and Steven C. H. Hoi. Instructblip: Towards general-purpose vision-language models with instruction tuning. In *Advances in Neural Information Processing Systems (NeurIPS)*, 2023.

Matt Deitke, Dustin Schwenk, Jordi Salvador, Luca Weihs, Oscar Michel, Eli VanderBilt, Ludwig Schmidt, Kiana Ehsani, Aniruddha Kembhavi, and Ali Farhadi. Objaverse: A universe of annotated 3d objects. In *Proceedings of the IEEE/CVF Conference on Computer Vision and Pattern Recognition (CVPR)*, pp. 13142–13153, 2023.

Soham Deshmukh, Benjamin Elizalde, Rita Singh, and Huaming Wang. Pengi: An audio language model for audio tasks. In *Advances in neural information processing systems (NeurIPS)*, 2023.

Alexey Dosovitskiy, Lucas Beyer, Alexander Kolesnikov, Dirk Weissenborn, Xiaohua Zhai, Thomas Unterthiner, Mostafa Dehghani, Matthias Minderer, Georg Heigold, Sylvain Gelly, Jakob Uszkoreit, and Neil Houlsby. An image is worth 16x16 words: Transformers for image recognition at scale. In *Proceedings of the International Conference on Learning Representations (ICLR)*, 2021.

Konstantinos Drossos, Samuel Lipping, and Tuomas Virtanen. Clotho: an audio captioning dataset. In *Proceedings of the IEEE International Conference on Acoustics, Speech, and Signal Processing (ICASSP)*, pp. 736–740, 2020.

Rohit Girdhar, Alaaeldin El-Nouby, Zhuang Liu, Mannat Singh, Kalyan Vasudev Alwala, Armand Joulin, and Ishan Misra. Imagebind one embedding space to bind them all. In *Proceedings of the IEEE/CVF Conference on Computer Vision and Pattern Recognition (CVPR)*, pp. 15180–15190, 2023.

Yuan Gong, Jin Yu, and James R. Glass. Vocalsound: A dataset for improving human vocal sounds recognition. In *Proceedings of the IEEE International Conference on Acoustics, Speech, and Signal Processing (ICASSP)*, pp. 151–155, 2022.

Yuan Gong, Hongyin Luo, Alexander H. Liu, Leonid Karlinsky, and James R. Glass. Listen, think, and understand. In *Proceedings of the International Conference on Learning Representations (ICLR)*, 2024.

Ian J Goodfellow, Mehdi Mirza, Da Xiao, Aaron Courville, and Yoshua Bengio. An empirical investigation of catastrophic forgetting in gradient-based neural networks. *arXiv preprint arXiv:1312.6211*, 2013.

Yash Goyal, Tejas Khot, Douglas Summers-Stay, Dhruv Batra, and Devi Parikh. Making the V in VQA matter: Elevating the role of image understanding in visual question answering. In *Proceedings of the IEEE/CVF Conference on Computer Vision and Pattern Recognition (CVPR)*, pp. 6325–6334, 2017.

Vipul Gupta, Santiago Akle Serrano, and Dennis DeCoste. Stochastic weight averaging in parallel: Large-batch training that generalizes well. In *Proceedings of the International Conference on Learning Representations (ICLR)*, 2020.

Danna Gurari, Qing Li, Abigale J Stangl, Anhong Guo, Chi Lin, Kristen Grauman, Jiebo Luo, and Jeffrey P Bigham. Vizwiz grand challenge: Answering visual questions from blind people. In *Proceedings of the IEEE/CVF Conference on Computer Vision and Pattern Recognition (CVPR)*, pp. 3608–3617, 2018.

Jiaming Han, Renrui Zhang, Wenqi Shao, Peng Gao, Peng Xu, Han Xiao, Kaipeng Zhang, Chris Liu, Song Wen, Ziyu Guo, et al. Imagebind-llm: Multi-modality instruction tuning. *arXiv preprint arXiv:2309.03905*, 2023.

Jiaming Han, Kaixiong Gong, Yiyuan Zhang, Jiaqi Wang, Kaipeng Zhang, Dahua Lin, Yu Qiao, Peng Gao, and Xiangyu Yue. Onellm: One framework to align all modalities with language. In *Proceedings of the IEEE/CVF Conference on Computer Vision and Pattern Recognition (CVPR)*, pp. 26584–26595, 2024.

Drew A Hudson and Christopher D Manning. Gqa: A new dataset for real-world visual reasoning and compositional question answering. In *Proceedings of the IEEE/CVF Conference on Computer Vision and Pattern Recognition (CVPR)*, pp. 6700–6709, 2019.

Gabriel Ilharco, Mitchell Wortsman, Samir Yitzhak Gadre, Shuran Song, Hannaneh Hajishirzi, Simon Kornblith, Ali Farhadi, and Ludwig Schmidt. Patching open-vocabulary models by interpolating weights. In *Advances in Neural Information Processing Systems (NeurIPS)*, 2022.

Gabriel Ilharco, Marco Túlio Ribeiro, Mitchell Wortsman, Ludwig Schmidt, Hannaneh Hajishirzi, and Ali Farhadi. Editing models with task arithmetic. In *Proceedings of the International Conference on Learning Representations (ICLR)*, 2023.

Biao Jiang, Xin Chen, Wen Liu, Jingyi Yu, Gang Yu, and Tao Chen. Motiongpt: Human motion as a foreign language. In *Advances in neural information processing systems (NeurIPS)*, 2023.

Jacob Devlin Ming-Wei Chang Kenton and Lee Kristina Toutanova. BERT: Pre-training of deep bidirectional transformers for language understanding. In *Proceedings of the Conference of the North American Chapter of the Association for Computational Linguistics: Human Language Technologies (NAACL-HLT)*, pp. 4171–4186, 2019.

Bo Li, Yuanhan Zhang, Liangyu Chen, Jinghao Wang, Jingkang Yang, and Ziwei Liu. Otter: A multi-modal model with in-context instruction tuning. *arXiv preprint arXiv:2305.03726*, 2023a.

Guangyao Li, Yake Wei, Yapeng Tian, Chenliang Xu, Ji-Rong Wen, and Di Hu. Learning to answer questions in dynamic audio-visual scenarios. In *Proceedings of the IEEE/CVF Conference on Computer Vision and Pattern Recognition (CVPR)*, pp. 19086–19096, 2022.

Junnan Li, Dongxu Li, Silvio Savarese, and Steven C. H. Hoi. BLIP-2: bootstrapping language-image pre-training with frozen image encoders and large language models. In *Proceedings of the International Conference on Machine Learning (ICML)*, pp. 19730–19742, 2023b.

Yifan Li, Yifan Du, Kun Zhou, Jinpeng Wang, Wayne Xin Zhao, and Ji-Rong Wen. Evaluating object hallucination in large vision-language models. In *Proceedings of the Conference on Empirical Methods in Natural Language Processing (EMNLP)*, pp. 292–305, 2023c.

Bin Lin, Bin Zhu, Yang Ye, Munan Ning, Peng Jin, and Li Yuan. Video-llava: Learning united visual representation by alignment before projection. *arXiv preprint arXiv:2311.10122*, 2023.

Samuel Lipping, Parthasaarathy Sudarsanam, Konstantinos Drossos, and Tuomas Virtanen. Clotho-aqa: A crowdsourced dataset for audio question answering. In *Proceedings of the European Signal Processing Conference (EUSIPCO)*, pp. 1140–1144, 2022.

Haotian Liu, Chunyuan Li, Qingyang Wu, and Yong Jae Lee. Visual instruction tuning. In *Advances in Neural Information Processing Systems (NeurIPS)*, 2023.

Haotian Liu, Chunyuan Li, Yuheng Li, and Yong Jae Lee. Improved baselines with visual instruction tuning. In *Proceedings of the IEEE/CVF Conference on Computer Vision and Pattern Recognition (CVPR)*, pp. 26296–26306, 2024.

Jinliang Lu, Ziliang Pang, Min Xiao, Yaochen Zhu, Rui Xia, and Jiajun Zhang. Merge, ensemble, and cooperate! a survey on collaborative strategies in the era of large language models. *arXiv preprint arXiv:2407.06089*, 2024.

Pan Lu, Swaroop Mishra, Tanglin Xia, Liang Qiu, Kai-Wei Chang, Song-Chun Zhu, Oyvind Tafjord, Peter Clark, and Ashwin Kalyan. Learn to explain: Multimodal reasoning via thought chains for science question answering. In *Advances in Neural Information Processing Systems (NeurIPS)*, volume 35, pp. 2507–2521, 2022.

Ruipu Luo, Ziwang Zhao, Min Yang, Junwei Dong, Da Li, Pengcheng Lu, Tao Wang, Linmei Hu, Minghui Qiu, and Zhongyu Wei. Valley: Video assistant with large language model enhanced ability. *arXiv preprint arXiv:2306.07207*, 2023.

Chenyang Lyu, Minghao Wu, Longyue Wang, Xinting Huang, Bingshuai Liu, Zefeng Du, Shuming Shi, and Zhaopeng Tu. Macaw-llm: Multi-modal language modeling with image, audio, video, and text integration. *arXiv preprint arXiv:2306.09093*, 2023.

Muhammad Maaz, Hanoona Abdul Rasheed, Salman Khan, and Fahad Khan. Video-chatgpt: Towards detailed video understanding via large vision and language models. In *Proceedings of the Annual Meeting of the Association for Computational Linguistics (ACL)*, 2024.

Kenneth Marino, Mohammad Rastegari, Ali Farhadi, and Roozbeh Mottaghi. Ok-vqa: A visual question answering benchmark requiring external knowledge. In *Proceedings of the IEEE/CVF Conference on Computer Vision and Pattern Recognition (CVPR)*, pp. 3195–3204, 2019.

Xinhao Mei, Chutong Meng, Haohe Liu, Qiuqiang Kong, Tom Ko, Chengqi Zhao, Mark D. Plumbley, Yuexian Zou, and Wenwu Wang. Wavcaps: A chatgpt-assisted weakly-labelled audio captioning dataset for audio-language multimodal research. *IEEE ACM Transactions on Audio, Speech, and Language Processing (TASLP)*, 32:3339–3354, 2024.

Annamaria Mesaros, Toni Heittola, Aleksandr Diment, Benjamin Elizalde, Ankit Shah, Emmanuel Vincent, Bhiksha Raj, and Tuomas Virtanen. DCASE2017 challenge setup: Tasks, datasets and baseline system. In *Proceedings of the Workshop on Detection and Classification of Acoustic Scenes and Events (DCASE)*, pp. 85–92, 2017.

Seungwhan Moon, Andrea Madotto, Zhaojiang Lin, Tushar Nagarajan, Matt Smith, Shashank Jain, Chun-Fu Yeh, Prakash Murugesan, Peyman Heidari, Yue Liu, et al. Anymal: An efficient and scalable any-modality augmented language model. *arXiv preprint arXiv:2309.16058*, 2023.

Artemis Panagopoulou, Le Xue, Ning Yu, Junnan Li, Dongxu Li, Shafiq Joty, Ran Xu, Silvio Savarese, Caiming Xiong, and Juan Carlos Niebles. X-instructblip: A framework for aligning x-modal instruction-aware representations to llms and emergent cross-modal reasoning. *arXiv preprint arXiv:2311.18799*, 2023.

Abhishek Panigrahi, Nikunj Saunshi, Haoyu Zhao, and Sanjeev Arora. Task-specific skill localization in fine-tuned language models. In *Proceedings of the International Conference on Machine Learning (ICML)*, pp. 27011–27033, 2023.

Colin Raffel, Noam Shazeer, Adam Roberts, Katherine Lee, Sharan Narang, Michael Matena, Yanqi Zhou, Wei Li, and Peter J. Liu. Exploring the limits of transfer learning with a unified text-to-text transformer. *Journal of Machine Learning Research (JMLR)*, 21:140:1–140:67, 2020.

Alexandre Ramé, Matthieu Kirchmeyer, Thibaud Rahier, Alain Rakotomamonjy, Patrick Gallinari, and Matthieu Cord. Diverse weight averaging for out-of-distribution generalization. In *Advances in Neural Information Processing Systems (NeurIPS)*, 2022.

Paul K Rubenstein, Chulayuth Asawaroengchai, Duc Dung Nguyen, Ankur Bapna, Zalán Borsos, Félix de Chaumont Quitry, Peter Chen, Dalia El Badawy, Wei Han, Eugene Kharitonov, et al. Audiopalm: A large language model that can speak and listen. *arXiv preprint arXiv:2306.12925*, 2023.

Mustafa Shukor, Corentin Dancette, Alexandre Ramé, and Matthieu Cord. Unival: Unified model for image, video, audio and language tasks. *Transactions on Machine Learning Research (TMLR)*, 2023, 2023.

Amanpreet Singh, Vivek Natarajan, Meet Shah, Yu Jiang, Xinlei Chen, Dhruv Batra, Devi Parikh, and Marcus Rohrbach. Towards vqa models that can read. In *Proceedings of the IEEE/CVF Conference on Computer Vision and Pattern Recognition (CVPR)*, pp. 8317–8326, 2019.

Yixuan Su, Tian Lan, Huayang Li, Jialu Xu, Yan Wang, and Deng Cai. Pandagpt: One model to instruction-follow them all. *arXiv preprint arXiv:2305.16355*, 2023.

Anirudh S. Sundar, Chao-Han Huck Yang, David M. Chan, Shalini Ghosh, Venkatesh Ravichandran, and Phani Sankar Nidadavolu. Multimodal attention merging for improved speech recognition and audio event classification. In *Proceedings of the Workshop on the IEEE International Conference on Acoustics, Speech, and Signal Processing (ICASSP)*, pp. 655–659, 2024.

Yi-Lin Sung, Linjie Li, Kevin Lin, Zhe Gan, Mohit Bansal, and Lijuan Wang. An empirical study of multimodal model merging. In *Proceedings of the Conference on Empirical Methods in Natural Language Processing (EMNLP)*, pp. 1563–1575, 2023.

Hugo Touvron, Louis Martin, Kevin Stone, Peter Albert, Amjad Almahairi, Yasmine Babaei, Nikolay Bashlykov, Soumya Batra, Prajjwal Bhargava, Shruti Bhosale, et al. Llama 2: Open foundation and fine-tuned chat models. *arXiv preprint arXiv:2307.09288*, 2023.

Fanqi Wan, Xinting Huang, Deng Cai, Xiaojun Quan, Wei Bi, and Shuming Shi. Knowledge fusion of large language models. In *Proceedings of the International Conference on Learning Representations (ICLR)*, 2024.

Ke Wang, Nikolaos Dimitriadis, Guillermo Ortiz-Jiménez, François Fleuret, and Pascal Frossard. Localizing task information for improved model merging and compression. In *Proceedings of the International Conference on Machine Learning (ICML)*, 2024.

Mitchell Wortsman, Gabriel Ilharco, Samir Yitzhak Gadre, Rebecca Roelofs, Raphael Gontijo Lopes, Ari S. Morcos, Hongseok Namkoong, Ali Farhadi, Yair Carmon, Simon Kornblith, and Ludwig Schmidt. Model soups: averaging weights of multiple fine-tuned models improves accuracy without increasing inference time. In *Proceedings of the International Conference on Machine Learning (ICML)*, pp. 23965–23998, 2022.

Chengyue Wu, Teng Wang, Yixiao Ge, Zeyu Lu, Ruisong Zhou, Ying Shan, and Ping Luo. π-tuning: Transferring multimodal foundation models with optimal multi-task interpolation. In *Proceedings of the International Conference on Machine Learning (ICML)*, pp. 37713–37727, 2023a.

Shengqiong Wu, Hao Fei, Leigang Qu, Wei Ji, and Tat-Seng Chua. Next-gpt: Any-to-any multimodal LLM. In *Proceedings of the International Conference on Machine Learning (ICML)*, 2024.

Tianyu Wu, Shizhu He, Jingping Liu, Siqi Sun, Kang Liu, Qing-Long Han, and Yang Tang. A brief overview of chatgpt: The history, status quo and potential future development. *IEEE CAA J. Autom. Sinica (JAS)*, 10(5): 1122–1136, 2023b.

Zhirong Wu, Shuran Song, Aditya Khosla, Fisher Yu, Linguang Zhang, Xiaoou Tang, and Jianxiong Xiao. 3d shapenets: A deep representation for volumetric shapes. In *Proceedings of the IEEE/CVF Conference on Computer Vision and Pattern Recognition (CVPR)*, pp. 1912–1920, 2015.

Jun Xu, Tao Mei, Ting Yao, and Yong Rui. Msr-vtt: A large video description dataset for bridging video and language. In *Proceedings of the IEEE/CVF Conference on Computer Vision and Pattern Recognition (CVPR)*, pp. 5288–5296, 2016.

Runsen Xu, Xiaolong Wang, Tai Wang, Yilun Chen, Jiangmiao Pang, and Dahua Lin. Pointllm: Empowering large language models to understand point clouds. In *Proceedings of the European Conference on Computer Vision (ECCV)*, 2024.

Prateek Yadav, Derek Tam, Leshem Choshen, Colin A. Raffel, and Mohit Bansal. Ties-merging: Resolving interference when merging models. In *Advances in Neural Information Processing Systems (NeurIPS)*, 2023.

Enneng Yang, Li Shen, Guibing Guo, Xingwei Wang, Xiaochun Cao, Jie Zhang, and Dacheng Tao. Model merging in llms, mllms, and beyond: Methods, theories, applications and opportunities. *arXiv preprint arXiv:2408.07666*, 2024.

Yibo Yang, Haobo Yuan, Xiangtai Li, Zhouchen Lin, Philip H. S. Torr, and Dacheng Tao. Neural collapse inspired feature-classifier alignment for few-shot class-incremental learning. In *Proceedings of the International Conference on Learning Representations (ICLR)*, 2023.

Qinghao Ye, Haiyang Xu, Guohai Xu, Jiabo Ye, Ming Yan, Yiyang Zhou, Junyang Wang, Anwen Hu, Pengcheng Shi, Yaya Shi, et al. mplug-owl: Modularization empowers large language models with multimodality. *arXiv preprint arXiv:2304.14178*, 2023.

Peter Young, Alice Lai, Micah Hodosh, and Julia Hockenmaier. From image descriptions to visual denotations: New similarity metrics for semantic inference over event descriptions. *Transactions of the Association for Computational Linguistics (TACL)*, 2:67–78, 2014.

Le Yu, Bowen Yu, Haiyang Yu, Fei Huang, and Yongbin Li. Language models are super mario: Absorbing abilities from homologous models as a free lunch. In *Proceedings of the International Conference on Machine Learning (ICML)*, 2024.

Zijia Zhao, Longteng Guo, Tongtian Yue, Sihan Chen, Shuai Shao, Xinxin Zhu, Zehuan Yuan, and Jing Liu. Chatbridge: Bridging modalities with large language model as a language catalyst. *arXiv preprint arXiv:2305.16103*, 2023.

Lianmin Zheng, Wei-Lin Chiang, Ying Sheng, Siyuan Zhuang, Zhanghao Wu, Yonghao Zhuang, Zi Lin, Zhuohan Li, Dacheng Li, Eric P. Xing, Hao Zhang, Joseph E. Gonzalez, and Ion Stoica. Judging llm-as-a-judge with mt-bench and chatbot arena. In *Advances in Neural Information Processing Systems (NeurIPS)*, 2023.

Bin Zhu, Bin Lin, Munan Ning, Yang Yan, Jiaxi Cui, Hongfa Wang, Yatian Pang, Wenhao Jiang, Junwu Zhang, Zongwei Li, Caiwan Zhang, Zhifeng Li, Wei Liu, and Li Yuan. Languagebind: Extending video-language pretraining to n-modality by language-based semantic alignment. In *Proceedings of the International Conference on Learning Representations (ICLR)*, 2024a.

Deyao Zhu, Jun Chen, Xiaoqian Shen, Xiang Li, and Mohamed Elhoseiny. Minigpt-4: Enhancing vision-language understanding with advanced large language models. In *Proceedings of the International Conference on Learning Representations (ICLR)*, 2024b.

Didi Zhu, Zhongyi Sun, Zexi Li, Tao Shen, Ke Yan, Shouhong Ding, Chao Wu, and Kun Kuang. Model tailor: Mitigating catastrophic forgetting in multi-modal large language models. In *Proceedings of the International Conference on Machine Learning (ICML)*, 2024c.

A Novelty and Contributions

Our research aims to achieve training-free multi-modality expansion and retention for LLMs through parameter merging and decoupling. We conduct a comparative analysis with existing relevant methods to demonstrate the innovation of our MMER approach.

Comparison with NaiveMC and DAMC frameworks. Our MMER approach is based on the NaiveMC framework (Chen et al., 2024) and employs a parameter dynamic decoupling strategy similar to that of the DAMC framework (Chen et al., 2024) to mitigate parameter conflicts in the merged MLLM. However, there are several key differences:

1. Compared to the NaiveMC framework, our MMER approach effectively enhances the multimodal performance of the merged MLLM.
2. Compared to the DAMC framework, our MMER approach employs a training-free parameter decoupling strategy instead of separating parameters during the initialization training of the MLLMs and achieves similar results. Additionally, MMER is additional compatible with full-parameter fine-tuned MLLMs, whereas DAMC is restricted to parameter-efficient fine-tuned MLLMs.
3. Compared to the NaiveMC and DAMC frameworks, our MMER approach retains the performance of the original MLLMs while also providing additional capabilities to mitigate catastrophic forgetting.

Our MMER approach integrates the strengths of the NaiveMC and DAMC frameworks, while additionally providing original performance retention capabilities.

Comparison with training-free model merging methods. Training-free model merging methods, such as TA (Ilharco et al., 2023), TIES (Yadav et al., 2023), and DARE (Yu et al., 2024), are primarily designed for merging models with identical architectures. Consequently, they must be combined with the NaiveMC framework to achieve multi-modality expansion for LLMs. These methods alleviate parameter conflicts in merged MLLMs to some extent, leading to performance enhancement. However, their overall effectiveness, both in terms of multimodal performance and retention of original performance, falls significantly short compared to our MMER approach.

Comparison with alignment and fine-tuning methods. Compared to methods (Chen et al., 2023a; Lyu et al., 2023; Han et al., 2024) that achieve multimodal expansion for LLMs by adding multiple new modality encoders or employing a unified multimodal encoder followed by alignment and fine-tuning, the advantages of our MMER approach are clear. MMER can effectively reuse a large number of MLLMs from the open-source community and merge them enabling multimodal expansion without the need for extensive resources and time spent on training models and constructing high-quality modality instruction data.

Comparison with TALL-masks. TALL-masks (Wang et al., 2024) is an information localization algorithm that, similar to our approach, compresses original parameters and subsequently approximates their restoration. However, there are several key differences:

1. From an algorithmic perspective, TALL-masks overlooks the Consistency of original and merged parameter signs. In contrast, we have addressed this aspect and demonstrated its effectiveness in our ablation experiments (See Table 5).
2. In terms of application scenarios, our MMER applies parameter merging and decoupling to the multimodal expansion for LLMs, enhancing their multimodal capabilities. Additionally, we utilize MMER to mitigate catastrophic forgetting. These aspects are not considered by TALL-masks.
3. Regarding the models utilized, the models used in our MMER approach are the 7B MLLMs across various modalities, while TALL-masks is applied to relatively smaller models within the same modality, such as T5 (Raffel et al., 2020) and ViT (Dosovitskiy et al., 2021).

B Implementation and Experimental Details

All our experiments are conducted on an NVIDIA 8×A800-SXM4-80GB machine.

B.1 Performance retention

Considering the varying modalities of each original MLLM and the different evaluation metrics for distinct tasks, we provide performance retention in our results to validate the method's capacity to retain original performance. The definition is as follows:

$$\text{Performance Retention} = \frac{1}{T}\sum_{t=1}^{T} \frac{\underset{x\sim\mu_t}{\text{metric}}\left[f_{\text{method}}(x)\right]}{\underset{x\sim\mu_t}{\text{metric}}\left[f_{\text{original}}(x)\right]} \tag{8}$$

The "metric" refers to various evaluation metrics, such as accuracy and captioning scores(e.g., BLEU, ROUGE).

B.2 Implementation Details of original Fine-tuned MLLMs

We utilize the same training data and components of each MLLM across the four modalities following NaiveMC (Chen et al., 2024). More details are presented in Table 6.

Table 6: Training data and components of MLLMs for different modalities.

Modality	Modality Encoder	Connector	Alignment Data	Fine-tuneing Data	Referenced Work
Image	CLIP-ViT-L-336px (Dosovitskiy et al., 2021)	MLP	LCS 558K (Xu et al., 2024)	LLaVA-mixed 665K (Xu et al., 2024)	LLaVA-1.5 (Liu et al., 2024)
Audio	BEATs-Iter3+ (Chen et al., 2023b)	Q-Former	WaveCaps 400K (Mei et al., 2024)	OpenAQA filtered 350K (Gong et al., 2024)	X-InstructBLIP (Panagopoulou et al., 2023)
Video	LanguageBind (Zhu et al., 2024a)	MLP	LCS 558K, Valley 702K (Luo et al., 2023)	Video-ChatGPT 100K (Maaz et al., 2024), LLaVA-mixed sampled 140K	Video-LLaVA (Lin et al., 2023)
Point Cloud	Point Encoder (Xu et al., 2024)	MLP	PointLLM brief description 660K (Xu et al., 2024)	Point complex instruction 70K (Xu et al., 2024)	PointLLM (Xu et al., 2024)

We adopt similar hyperparameters following previous works (Chen et al., 2024; Liu et al., 2024; Panagopoulou et al., 2023; Lin et al., 2023; Xu et al., 2024). During the alignment stage, only the parameters in the connectors are trainable. In the fine-tuning stage, we tune all connector parameters and base LLM parameters. For training efficiency, we utilize DeepSpeed Zero Optimization Stage 3. Detailed data are presented in the Table 7.

B.3 Baseline Details

In this section, we provide a detailed overview of the six baselines included in our experiments:

- **Original MLLMs** means that each MLLM is evaluated on its corresponding modality benchmarks to demonstrate its original performance, but they cannot perform cross-modal tasks simultaneously.
- **NaiveMC framework** (Chen et al., 2024) combines modality-specific encoders from multiple MLLMs into the merged LLM, which is obtained by averaging the parameters of multiple LLMs from these MLLMs. The averaging merging strategy can be replaced by other model merging methods.
- **TA** (Ilharco et al., 2023) initially defines the concept of *task vector* and employs arithmetic operations for model merging, model forgetting, and support multi-task learning, etc. The final model is formed by scaling and adding task vectors to the initial model, represented mathematically as $\theta_m = \theta_{\text{init}} + \lambda \cdot \sum_{t=1}^{n} \tau_t$.

Table 7: Hyperparameters of different MLLMs.

Stage	Hyperparameter	Image	Audio	Video	Point Cloud
Alignment-State	Batch size	256	256	256	128
	LR	1e-3	1e-3	1e-3	2e-3
	LR Schedule	cosine decay			
	Warmup Ratio	0.03			
	Epoch	1	1	1	3
Fine-tuning-Stage	Batch size	128	64	128	64
	LR	2e-5	1e-5	2e-5	2e-5
	LR Schedule	cosine decay			
	Warmup Ratio	0.03			
	Epoch	1	3	1	3

- **TIES** (Yadav et al., 2023) improves upon TA (Ilharco et al., 2023) by further mitigating parameter interference. It first prunes redundant parameters to retain the most important ones. When encountering conflicts in parameter signs during merging, it selects and merges parameters with the majority sign while ignoring those with minority signs.
- **DARE** (Yu et al., 2024) proposes a preprocessing step to address parameters conflict. This method randomly discards the majority of the delta parameters while scaling the remaining ones by $\theta' = \theta \cdot (1/(1-p))$ where p is the proportion of dropped delta parameters.
- **Model Tailor** (Zhu et al., 2024c) identifies the key parameters fine-tuned on the new tasks within the MLLM and integrates them into the original MLLM, thereby retaining the performance on previous tasks while adapting to new tasks.

C Storage Cost Calculation

This section details the calculation of storage costs for MMER approach and the relevant methods mentioned above. Let N, P, P', and P^* represent the number of original MLLMs, the total parameters of the LLMs, the number of the modality-specific component parameters, and the number of additional trainable parameters of parameter-efficient fine-tuning methods, respectively. Assuming each float parameter occupies 32 bits, the storage cost for these methods across N original MLLMs is calculated as follows:

- Original fine-tuned models: $32N(P+P')$. $32(P+P')$ represents the number of parameters contained in a single MLLM.
- NaiveMC framework: $32P + 32NP'$. Stores a merged LLM and N modality-specific components.
- DAMC framework: $32P + 32NP' + 2N(32P^*)$. Stores a merged LLM and N modality-specific components. $2N(32P^*)$ represents the need to store an additional $2N$ trainable parameters of parameter-efficient fine-tuning methods for parameter separation.
- NaiveMC wit TA / TIES / DARE: $32P + 32NP'$. Same as the NaiveMC framework.
- MMER: $64P + 32NP' + NP$. $64P$ is for storing the parameters of a base LLM and a merged task vector, while $32NP'$ indicates N modality-specific components. Additionally, NP denotes the storage for N binary masks.

D More Details about Experiments

D.1 More Results

We supplement the results of mainstream MLLMs, such as ImageBind-LLM and OneLLM, on multimodal benchmarks in Table 8 and observe that MMER achieves superior performance compared to them.

D.2 Detailed Results

In this section, we present detailed results from the multi-modality retention and mitigating catastrophic forgetting experiments. The results of various baselines for seven image tasks are shown in Table 9, two point cloud tasks in Table 10, three audio tasks and two video tasks in Table 11, three multimodal tasks in Table 12, and the last two new tasks in Table 13.

Table 8: The results of mainstream MLLMs on multimodal benchmarks

Task (→)	**ModelNet40**	**MUSCI-AVQA**			**MCUB**					Avg
Method (↓)	PI-T	IA-T	VI-T	VA-T	AVI-T	AVP-T	AIP-T	VIP-T	AVIP-T	
OneLLM-7B (Han et al., 2024)	-	44.64	45.48	47.60	-	-	-	-	-	-
ImageBind-LLM(Han et al., 2023)	39.86	36.54	38.76	39.72	35.20	31.40	33.40	31.80	32.93	35.51
X-InstructBLIP(Panagopoulou et al., 2023)	57.93	40.71	41.23	48.34	41.40	25.20	21.20	29.40	27.94	37.04
MMER (ours)	**62.15**	**47.25**	**51.27**	**51.77**	**56.48**	**59.31**	**65.59**	**56.00**	**61.63**	**56.82**

Table 9: Results for each method on seven image tasks. All tasks are Question-Answering tasks.

Task (→)	**7 Image Tasks**						
	VQAv2	GQA	TextVQA	VizWiz	ScienceQA	POPE	OK-VQA
Method (↓)	Acc.	Acc.	Acc.	Acc.	Acc.	Acc.	Acc.
Original MLLMs	78.11	61.52	55.89	51.51	71.12	86.17	31.33
MMER (ours)	77.95	61.85	55.74	52.26	71.16	86.58	31.27
–Multi-Modality Retention							
NaiveMC [ACL2024] (Chen et al., 2024)	59.73	45.83	42.29	47.87	68.52	79.41	24.28
TA [ICLR23] (Ilharco et al., 2023)	62.71	48.86	45.20	49.47	70.04	82.38	25.56
TIES [NeurIPS23] (Yadav et al., 2023)	61.78	48.23	44.60	48.67	69.05	81.21	25.13
NaiveMC (w/ DARE[ICML2024] (Yu et al., 2024))	60.91	46.62	42.88	49.04	70.09	81.08	24.62
TA (w/ DARE)	63.65	49.25	45.74	49.82	70.87	83.12	25.82
TIES (w/ DARE)	62.54	48.73	45.38	49.15	69.78	82.17	25.39
–Mitigating Catastrophic Forgetting							
Fine-tune on Flickr30k	72.27	54.19	46.10	52.88	70.22	76.78	28.31
MMER-Clotho-AQA	77.87	61.59	55.51	51.88	71.16	86.24	31.14
MMER-Flickr30k	77.75	61.43	55.41	52.72	71.75	85.72	31.07
MMER-Clotho-AQA+Flickr30k	77.32	61.33	55.23	52.33	71.02	85.43	30.94

E Qualitative Results

We provide qualitative results in Figure 6 and 7. These results demonstrate the capability of the merged MLLM constructed by our MMER approach to understand and reason with multimodal inputs.

F Prompt for Evaluation

We present the evaluation prompts for each benchmark in Table 14. To denote the inputs for various modalities, we use "<image>", "<audio>", "<video>", and "<point>" to represent image, audio, video, and point cloud modalities, respectively.

Table 10: Results for each method on two point cloud tasks. Among them, ModelNet40 is a classification task, while Objavers is a captioning task.

Task (→)	2 Point Tasks					
	ModelNet40	Objavers				
Method (↓)	Acc.	BLEU-1	ROUGE-L	METEOR	Sentence-BERT	SimCSE
Original MLLMs	21.27	4.73	8.51	12.02	44.18	46.31
MMER (ours)	22.49	5.06	8.53	11.90	43.72	46.51
–Multi-Modality Retention						
NaiveMC [ACL2024] (Chen et al., 2024)	20.49	4.43	8.24	11.37	43.22	45.97
TA [ICLR23] (Ilharco et al., 2023)	21.02	4.69	8.46	11.73	43.55	46.38
TIES [NeurIPS23] (Yadav et al., 2023)	20.83	4.55	8.39	11.60	43.29	46.27
NaiveMC (w/ DARE[ICML2024] (Yu et al., 2024))	20.77	4.41	8.38	11.59	43.47	46.28
TA (w/ DARE)	21.25	4.81	8.49	11.82	43.67	46.42
TIES (w/ DARE)	20.98	4.62	8.31	11.47	43.14	46.28
–Mitigating Catastrophic Forgetting						
MMER-Clotho-AQA	21.87	4.92	8.46	11.52	43.55	46.28
MMER-Flickr30k	22.03	5.08	8.55	11.63	43.61	46.36
MMER-Clotho-AQA+Flickr30k	21.56	4.98	8.39	11.38	43.34	46.02

Table 11: Results for each method on three audio tasks and two video tasks. Among them, TUT, VocalSound, MSVD, and MSRVTT are the classification tasks, while Clotho is a captioning task.

Task (→)	3 Audio Tasks					2 Video Tasks	
	TUT	VocalSound	Clotho			MSVD	MSRVTT
Method (↓)	Acc.	Acc.	CIDEr	SPICE	SPIDEr	Acc.	Acc.
Original MLLMs	22.23	27.19	38.63	11.98	25.29	48.40	31.18
MMER (ours)	34.14	42.88	38.49	11.93	25.18	48.12	30.43
–Multi-Modality Retention							
NaiveMC [ACL2024] (Chen et al., 2024)	29.50	31.80	37.56	11.61	24.61	44.53	29.31
TA [ICLR23] (Ilharco et al., 2023)	30.64	33.12	37.69	11.67	24.69	45.61	29.54
TIES [NeurIPS23] (Yadav et al., 2023)	30.87	33.42	37.89	11.72	24.78	45.88	29.74
NaiveMC (w/ DARE[ICML2024] (Yu et al., 2024))	30.50	32.75	37.75	11.66	24.74	45.69	29.58
TA (w/ DARE)	30.98	33.90	37.87	11.69	24.89	45.51	29.54
TIES (w/ DARE)	31.59	34.45	37.96	11.87	24.92	46.07	29.93
–Mitigating Catastrophic Forgetting							
Fine-tune on Clotho-AQA	6.98	17.65	30.02	9.40	20.04	-	-
MMER-Clotho-AQA	34.01	42.45	38.37	11.89	25.11	48.04	30.29
MMER-Flickr30k	33.41	41.94	38.10	11.81	24.98	47.74	30.05
MMER-Clotho-AQA+Flickr30k	33.54	41.83	37.97	11.76	24.92	47.38	29.67

Table 12: Results of the mitigating catastrophic forgetting experiments for three MMER variants on multimodal tasks with different combinations of video (V), image (I), audio (A), point cloud (P), and text (T) inputs.

Task (→)	ModelNet40	MUSCI-AVQA			MCUB				
Method (↓)	PI-T	IA-T	VI-T	VA-T	AVI-T	AVP-T	AIP-T	VIP-T	AVIP-T
MMER-Clotho-AQA	61.98	47.01	51.22	51.43	56.08	59.11	65.08	55.80	61.08
MMER-Flickr30k	61.84	46.92	51.05	51.56	56.28	58.90	65.08	55.40	60.93
MMER-Clotho-AQA+Flickr30k	61.33	46.48	50.61	51.17	55.68	57.93	64.17	55.20	60.42

Table 13: Results of the mitigating catastrophic forgetting experiments for each method on two **new tasks**. Among them, Clotho-AQA is a Question-Answering task, while Flickr30k is a captioning task.

Task (→)	Clotho-AQA	Flickr30k						
Method (↓)	Acc.	CIDEr	METEOR	BLEU-1	BLEU-2	BLEU-3	BLEU-4	ROUGE
Original MLLMs	49.40	80.27	25.62	73.29	55.81	41.11	29.66	53.11
Fine-tune on Clotho-AQA	57.80	-	-	-	-	-	-	-
Fine-tune on Flickr30k	-	94.25	27.74	78.27	62.24	47.99	36.50	57.04
MMER (ours)	49.28	79.56	25.56	73.11	55.62	40.83	29.49	52.82
MMER-Clotho-AQA	57.71	79.72	25.51	73.04	55.48	40.72	29.33	52.77
MMER-Flickr30k	48.94	92.74	27.58	77.93	61.69	47.36	36.02	56.27
MMER-Clotho-AQA+Flickr30k	57.52	92.09	27.29	77.22	61.11	46.86	35.62	55.72

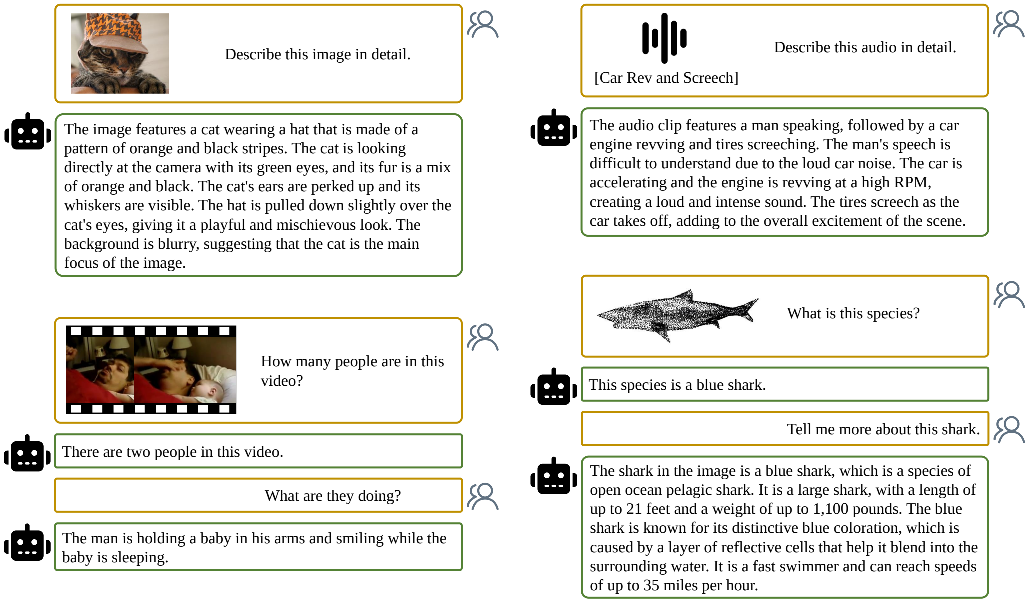

Describe this image in detail.

The image features a cat wearing a hat that is made of a pattern of orange and black stripes. The cat is looking directly at the camera with its green eyes, and its fur is a mix of orange and black. The cat's ears are perked up and its whiskers are visible. The hat is pulled down slightly over the cat's eyes, giving it a playful and mischievous look. The background is blurry, suggesting that the cat is the main focus of the image.

How many people are in this video?

There are two people in this video.

What are they doing?

The man is holding a baby in his arms and smiling while the baby is sleeping.

Describe this audio in detail.

The audio clip features a man speaking, followed by a car engine revving and tires screeching. The man's speech is difficult to understand due to the loud car noise. The car is accelerating and the engine is revving at a high RPM, creating a loud and intense sound. The tires screech as the car takes off, adding to the overall excitement of the scene.

What is this species?

This species is a blue shark.

Tell me more about this shark.

The shark in the image is a blue shark, which is a species of open ocean pelagic shark. It is a large shark, with a length of up to 21 feet and a weight of up to 1,100 pounds. The blue shark is known for its distinctive blue coloration, which is caused by a layer of reflective cells that help it blend into the surrounding water. It is a fast swimmer and can reach speeds of up to 35 miles per hour.

Figure 6: Qualitative results.

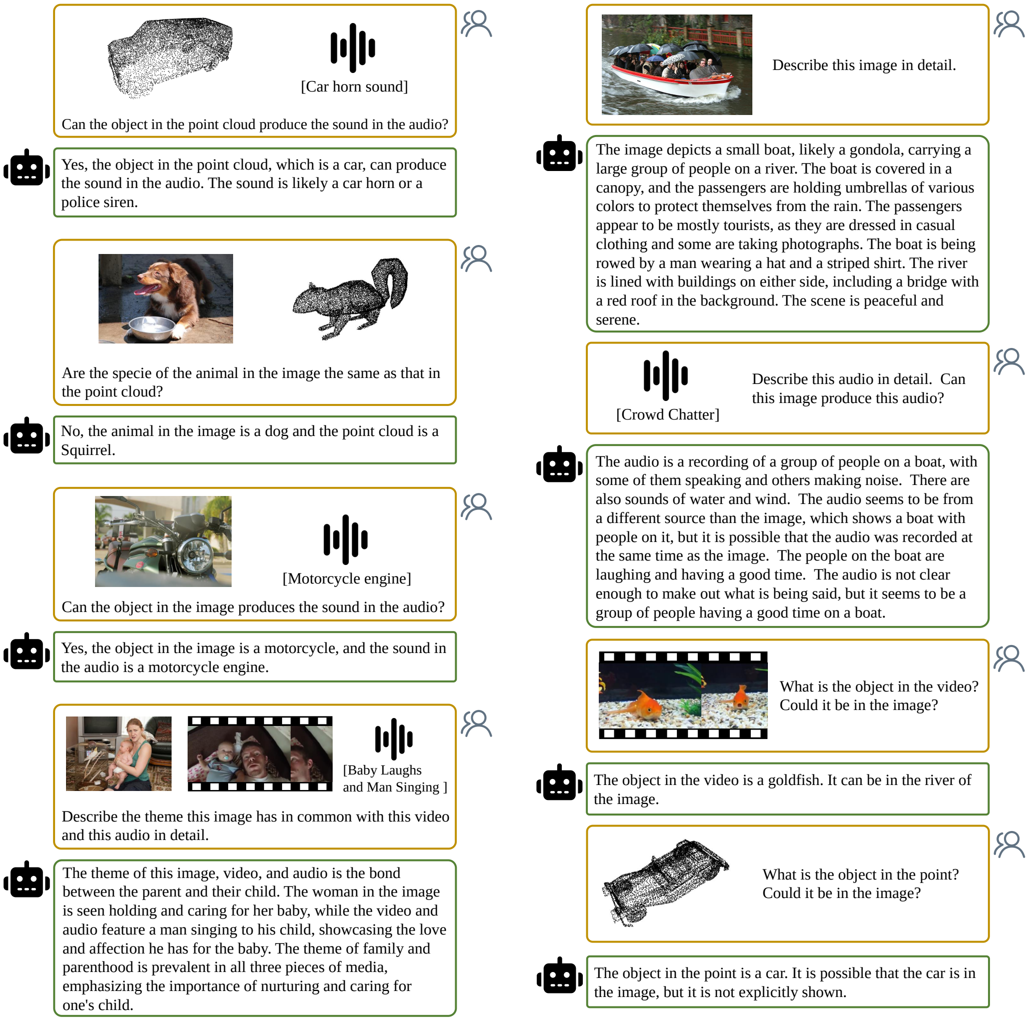

Can the object in the point cloud produce the sound in the audio?

Yes, the object in the point cloud, which is a car, can produce the sound in the audio. The sound is likely a car horn or a police siren.

Are the specie of the animal in the image the same as that in the point cloud?

No, the animal in the image is a dog and the point cloud is a Squirrel.

Can the object in the image produces the sound in the audio?

Yes, the object in the image is a motorcycle, and the sound in the audio is a motorcycle engine.

Describe the theme this image has in common with this video and this audio in detail.

The theme of this image, video, and audio is the bond between the parent and their child. The woman in the image is seen holding and caring for her baby, while the video and audio feature a man singing to his child, showcasing the love and affection he has for the baby. The theme of family and parenthood is prevalent in all three pieces of media, emphasizing the importance of nurturing and caring for one's child.

Describe this image in detail.

The image depicts a small boat, likely a gondola, carrying a large group of people on a river. The boat is covered in a canopy, and the passengers are holding umbrellas of various colors to protect themselves from the rain. The passengers appear to be mostly tourists, as they are dressed in casual clothing and some are taking photographs. The boat is being rowed by a man wearing a hat and a striped shirt. The river is lined with buildings on either side, including a bridge with a red roof in the background. The scene is peaceful and serene.

Describe this audio in detail. Can this image produce this audio?

The audio is a recording of a group of people on a boat, with some of them speaking and others making noise. There are also sounds of water and wind. The audio seems to be from a different source than the image, which shows a boat with people on it, but it is possible that the audio was recorded at the same time as the image. The people on the boat are laughing and having a good time. The audio is not clear enough to make out what is being said, but it seems to be a group of people having a good time on a boat.

What is the object in the video? Could it be in the image?

The object in the video is a goldfish. It can be in the river of the image.

What is the object in the point? Could it be in the image?

The object in the point is a car. It is possible that the car is in the image, but it is not explicitly shown.

Figure 7: Qualitative results.

Table 14: Prompt Template for different evaluation benchmarks.

Benchmark	Modality	Prompt Template
MCUB	AVI-T	Based on four input entities:\nimage <image>\naudio <audio>\nvideo <video>\n {Question} {Options} Answer with the option's letter from the given choices directly.
	AVP-T	Based on four input entities:\naudio <audio>\nvideo <video>\npoint <point>\n {Question} {Options} Answer with the option's letter from the given choices directly.
	VIP-T	Based on four input entities:\nimage <image>\nvideo <video>\npoint <point>\n {Question} {Options} Answer with the option's letter from the given choices directly.
	AIP-T	Based on three input entities:\nimage <image>\naudio <audio>\npoint <point>\n {Question} {Options} Answer with the option's letter from the given choices directly.
	AVIP-T	Based on four input entities:\nimage <image>\naudio <audio>\nvideo <video>\npoint <point>\n {Question} {Options} Answer with the option's letter from the given choices directly.
MUSIC-AVQA	VI-T	Based on the video <video> and image <image>\n{Question} \nAnswer the question using a single word.
	VA-T	Based on the video <video> and audio <audio>\n{Question} \nAnswer the question using a single word.
	IA-T	Based on the image <image> and audio <audio>\n{Question} \nAnswer the question using a single word.
ModelNet40	PI-T	Based on rendered image <image> and point cloud <point>\nWhat is this? Select from these objects: {Options} Answer the question using a single word.
	I-T	<point>\nWhat is this? Select from these objects: {Options} Answer the question using a single word.
Objaverse	I-T	<point>\nOffer a clear and concise description of this point cloud object.
VocalSound & TUT	A-T	<audio>\nWhich of the following categories does this audio belong to? {Options} Answer the question using a single word.
Clotho	A-T	<audio>\nDescribe this audio in detail.
Clotho-AQA	A-T	<audio>\n{Question}\nAnswer the question using a single word or phrase.
MSRVTT & MSVD	V-T	<video>\n{Question}\nAnswer the question using a single word or phrase.
VQAv2 & GQA & POPE & OK-VQA	I-T	<image>\n{Question}\nAnswer the question using a single word or phrase.
Textvqa	I-T	<image>\n{Question}\nReference OCR token: {Options}\nAnswer the question using a single word or phrase.
VizWiz	I-T	<image>\n{Question}\nWhen the provided information is insufficient, respond with 'Unanswerable'.\nAnswer the question using a single word or phrase.
ScienceQA	I-T	<image>\n{Context}\n{Question}\nChoose the most likely ratio. {Options}
Flickr30k	I-T	<image>\nDescribe this image using one or more simple sentences.